

## Comparison of two methods to assess heterogeneity of water flow in soils

Ľubomír Lichner<sup>\*1</sup>, Jaromír Dušek<sup>2</sup>, Louis W. Dekker<sup>3</sup>, Natalia Zhukova<sup>4</sup>,  
Pavol Faško<sup>5</sup>, Ladislav Holko<sup>1</sup>, Miloslav Šír<sup>6</sup>

<sup>1</sup> Institute of Hydrology, Slovak Academy of Sciences, Račianska 75, 831 02 Bratislava, Slovakia.

<sup>2</sup> Czech Technical University in Prague, Faculty of Civil Engineering, Thákurova 7, 166 29 Prague, Czech Republic.

<sup>3</sup> Wageningen University and Research Center, Alterra, Soil Science Center, P.O. Box 47, 6700 AA Wageningen, The Netherlands.

<sup>4</sup> M. Nodia Institute of Geophysics, 1 Alexidze str., 0193 Tbilisi, Georgia.

<sup>5</sup> Slovak Hydrometeorological Institute, Jeséniova 17, 833 15 Bratislava, Slovakia.

<sup>6</sup> Institute of Hydrodynamics, Academy of Sciences of the Czech Republic, Pod Patankou 30/5, 166 12 Prague, Czech Republic.

\* Corresponding author. Tel.: +421 2 49268227. Fax: +421 2 44259404. E-mail: [lichner@uh.savba.sk](mailto:lichner@uh.savba.sk)

**Abstract:** The heterogeneity of water flow and solute transport was assessed during radioactive tracer infiltration experiment in a black clay loam soil using modified methods to estimate the effective cross section (ECS) and the degree of preferential flow (DPF). The results of field and numerical experiments showed that these parameters characterized the heterogeneity of water flow in the soils unequivocally. The ECS decreases non-linearly and the DPF increases linearly with an increase of the bypassing ratio (ratio of macropore flow rate to total flow rate). The ECS decreased and the DPF increased with depth, which suggests an increase in the heterogeneity of water flow with depth. The plot of the DPF against ECS values calculated from the tracer experiment data was consistent with the relationship obtained by the numerical simulation assuming preferential flow in the neighbourhood of three probes.

**Keywords:** Degree of preferential flow; Effective cross section; Preferential flow in soil; Infiltration experiment; Radioactive tracer technique.

**Abbreviations:** BR, bypassing ratio; DPF, degree of preferential flow; ECS, effective cross section; FCA, fraction of cross-sectional area; FTWC, fraction of total water content change; TDR, time domain reflectometry.

### INTRODUCTION

The frequency and intensity of heavy rains following long dry and hot spells are increasing (Hardy, 2003), leading to surface runoff, soil erosion, and worsening stream water quality (Pekárová et al., 2012). In well-structured, loamy and clayey soils, water and even reactive solutes, adsorbed on small soil particles, might be channelled through larger pores (macropores) without penetrating into the fine porous matrix (Edwards et al., 1993; Shipitalo et al., 2000; Vogel et al., 2007). Once ponding has been initiated on the soil matrix, surface runoff may be generated at rainfall intensities less than the saturated hydraulic conductivity of the soil (Smettem, 2009).

The flow pathways of water through field soils are in many cases highly irregular, as it was demonstrated by dye tracer infiltration experiments (e.g., Flury et al., 1994; Dohnal et al., 2009; Homolák et al., 2009). Probably the first attempt to quantify the heterogeneity of water flow in a soil was made by Bouma et al. (1978). They investigated the flow of water through cores of dry cracked clay soil in the laboratory and showed that water applied to the surface at rates higher than the infiltration rate into the surface soil pedes could pass rapidly down the cracks and other channels (*syn.* macropores) bypassing the matrix of the soil (*syn.* micropores). The degree of short-circuiting was calculated as the ratio of the outflow rate to the application rate. The same method was later used by Kneale and White (1984), who introduced the so-called bypassing ratio (BR), which is a ratio of the rate of macropore flow to the rate of total (macropore and matrix) flow.

Lichner (1997) and Lichner et al. (1999) presented a radioactive tracer technique for *in situ* measurement of BR. First, radioactive iodine <sup>131</sup>I tracer was applied with water infiltration at a rate slightly lower than the infiltration rate into the soil

matrix, and the tracer front was established in the soil matrix at a depth of about 50 cm. Then, application of tracer-free water followed at a rate  $v$  higher than the infiltration rate into the soil matrix, and the vertical displacement of the tracer front was recorded using a probe inserted vertically. As the displacement  $h$  was caused by water moving in the soil matrix only, the bypassing ratio was calculated from equation:  $BR = 1 - h n_{ef} / v$ , where  $n_{ef}$  is the effective soil porosity.

To quantify the heterogeneity of water flow in soils, Täumer et al. (2006) proposed to use the effective cross section (ECS). ECS was estimated by fitting the standard Beta function to the cumulative values of the water content change (measured with the time domain reflectometry (TDR) sensors) over a horizontal cross section at certain depth. They defined ECS as the fraction of the total area that corresponds to 90% of water content change at a given depth.

The method for estimation of ECS was later modified by Lichner et al. (2011, 2013) for conditions of dye tracer infiltration experiment. Lichner et al. (2011, 2013) also introduced the degree of preferential flow (DPF) to quantify the heterogeneity of water flow in soils. The DPF was estimated by fitting the Beta function to the cumulative values of the water content change over the fraction of cross-sectional area. They defined DPF as the area between the Beta distribution curve and the straight line representing homogeneous water flow.

The objective of this study was to use and compare the ECS and DPF methods to quantify the flow regime during a radioactive tracer infiltration experiment. In addition, numerical experiments, in which we considered water flow regimes with different patterns, were proposed to evaluate the ECS and DPF parameters.

## MATERIALS AND METHODS

### Study site

The field site was located in the Danubian lowland of southwestern Slovakia. The Danubian lowland is a large (1260 km<sup>2</sup>) agricultural area, with the underlying aquifer containing about 10 km<sup>3</sup> of freshwater. A large part of the region is a unique inland delta of the Danube river, very important as a groundwater reservoir. Due to the shallow groundwater table, which rises up to 50 cm below the soil surface, the risk of groundwater pollution from agrochemicals is high. The climate of the studied region is characterized as transitional between temperate oceanic and continental with moderate precipitation. The climate tends to consist of long hot and dry spells interspersed with intense rainfalls (Faško et al., 2008), which can be met during the growing season. Daily precipitation ranging from 71 mm to 152 mm were observed e.g., at Siladice near Pezinok on 4 May 2012, at Pezinok-Myslenice on 10 July 1999, and at Komárno on 28 September 1998.

The study area was located at the Experimental Station of Research Institute of Irrigation at Most pri Bratislave village (48° 08' 27" N, 17° 14' 41" E). The station is about 133 m a.s.l. The average annual air temperature is 9.7°C, the average annual precipitation is 554 mm. The soil is a Chernozem (WRB, 2006) that has a clay loam texture (Soil Survey Division Staff, 1993). The soil profile consists of three relatively homogeneous horizons. Physical and chemical properties of the surface horizon were as follows: clay/loam/sand content was 53/46/1%, CaCO<sub>3</sub> content 11.2%, C<sub>org</sub> content 1.9%, pH (H<sub>2</sub>O) 8.2, and pH (KCl) 7.8.

### Radioactive tracer experiment

An original radioactive tracer technique (Lichner, 1990, 1992) was used to measure the tracer distribution in the soil at the study site. The radioactive tracer technique is rapid, able to locate heterogeneities in field soils, and suitable for performing replicate measurements at the same place (Alaoui et al., 1997). The measuring probe (Fig. 1) consists of a duralumin tube (3) with a Geiger-Müller (G-M) detector and an analogue interface unit (1), connected to the nuclear analyser (2) with a coaxial cable. The G-M detector can be placed in any desired position (scanning the probe) up to a depth of 1.5 m. The tubes (outer diameter 10-mm, inner diameter 8-mm, and length 1.5-m) were inserted vertically from the surface into the holes made into the soil by a 10 mm diameter steel rod. The steel bands served for demarcation of studied plots (4). Conical soil sealing (5) was required for each vertical probe to prevent water from bypassing the probe, as earlier assessed by a dye-staining test with Methylene Blue. Owing to its small size (21-mm length and 6.3-mm diameter) the G-M detector can be considered as a point detector. Despite the small dose of radioactive tracer used during the experiment, strict safety measures have to be followed as contamination by <sup>131</sup>I may result in destruction of thyroid tissue.

The radioactive tracer technique takes advantage of the nuclides emitting gamma radiation. The radioactive iodine <sup>131</sup>I (with the half-life time of 8.04 days and chemical form Na<sup>131</sup>I) was used as a tracer in this study. Recent research confirmed older findings that iodide cannot be considered as a non-reactive tracer because it is immobilized in soils in the form of organically bound iodine (Behrens, 1982) through the laccase-catalyzed oxidation (Seki et al., 2013). It was found that iodide was fully transformed into organic forms after 1 day of incubation in highly organic soils and was fully transformed in the

studied soils after 60 days (Shetaya, 2011). Therefore, the NaI solution was added in our experiment as a carrier to prevent <sup>131</sup>I from incorporation into organic compound and field micro-organisms. To reduce the irradiation loading, a few drops of the Na<sup>131</sup>I tracer with activity of about 10 MBq were trickled by syringe into the annulus with the diameter of about 10 cm around the probe.

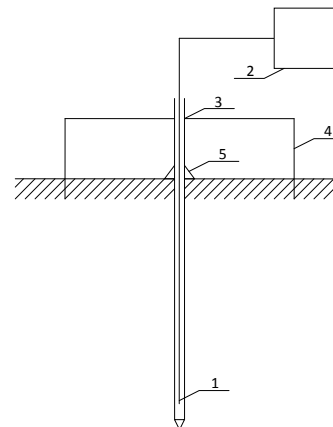


**Fig. 1.** Scheme of the field experiment set-up: 1 – Geiger-Müller detector, 2 – nuclear analyser, 3 – duralumin tube, 4 – steel bands demarcating the studied plot, 5 – seal made of clay-loam soil (Lichner, 1990, 1995).

The experiment was performed from 30 April to 1 May 1993. The measurements were carried out at a 1.5 m x 3.5 m plot in the field sown with spring barley (Lichner, 1995). Eight probes (4 at each line) were placed uniformly at two 3-m lines at a distance of 1 m and inserted into the soil to a depth of 1.5 m. After the application of Na<sup>131</sup>I and NaI solution, the plot was water irrigated at a rate  $v = 10 \text{ mm h}^{-1}$  for 10 hours. The irrigation was then interrupted for 12 hours to allow water and tracer redistribution within the soil profile. Following this interruption, another 100 mm of water was applied within 10 hours. The counting rates  $n_{mi}$  were measured in each probe as a function of depth  $z$  for cumulative water inputs  $I = 40 \text{ mm}$ ,  $100 \text{ mm}$ , and  $200 \text{ mm}$ . The measurement increments were 10 cm with the exception of the surface, where the measurement at  $z = 0$  was substituted with the measurement at  $z = 5 \text{ cm}$ . Finally, the corrected counting rates  $n_{ti}$  and relative counting rates  $n_{ri}$  in the probe  $i$  were calculated from:

$$n_{ti} = (n_{mi} - n_b) \exp(-0.693t/T)$$

$$\text{with } n_{ri} = n_{ti} / \sum_{z_1}^{z_N} n_{ti}, \quad (1)$$

where  $n_b$  is the counting rate of the background,  $t$  is the time elapsed after the start of tracer application,  $T$  is the tracer half-life time, and  $N$  is the number of measurement increments.

### Quantification of water flow heterogeneity

The effective cross section was calculated according to the method proposed by Täumer et al. (2006). They used the soil water content change estimated from TDR measurements for the calculation of the ECS. In the present study, the ECS was calculated from the relative counting rates  $n_r$  (assumed to be proportional to the soil water content change) measured at several depths of the soil profile. The fraction of total water content change  $f_i$  was calculated for each probe as:

$$f_i = n_{ri} / \sum_{i=1}^M n_{ri} \quad \text{with} \quad \sum_{i=1}^M f_i = 1, \quad (2)$$

where  $M$  is the number of probes. The fraction of total water content change (FTWC) is the ratio between the soil water content change in the close neighbourhood (circle with radius of about 10 cm) of the probe  $i$  and the total water content change at that depth estimated as the sum of total water content changes in all probes. The fractions  $f_i$  were ranked in descending order and presented against the fraction of cross-sectional area, FCA. The standard Beta function is defined as:

$$p(x; \alpha, \beta) = \frac{\Gamma(\alpha + \beta)}{\Gamma(\alpha)\Gamma(\beta)} x^{\alpha-1} (1-x)^{\beta-1}, \quad (3)$$

where  $\Gamma$  is the Gamma function and  $\alpha$  and  $\beta$  are free parameters which are assumed to be greater than zero. The Beta function was fitted to the experimental FTWC-FCA relationship using a non-linear, least-square fitting scheme which provided the optimized  $\alpha$  and  $\beta$  parameters. The fitted curve expresses the water content change as a function of the area. According to the definition in Täumer et al. (2006), the effective cross section was estimated as the fraction of the total area that corresponds to the 90% of water content change at the studied depth. Small values of the ECS suggest high degree of heterogeneity of water flow.

The degree of preferential flow is equal to the area between the Beta function fitted to the FTWC-FCA plot and the straight line representing homogeneous (piston) water flow. The DPF was calculated from (Lichner et al., 2011):

$$\text{DPF} = \int_{x=0}^1 p(x; \alpha, \beta) - 0.5. \quad (4)$$

The value of DPF can change from 0 for piston flow to almost 0.5 for the case when all water flow in the soil is realized through a narrow preferential path (e.g., a crack in heavy clay soil).

### Numerical experiments

To assess the performance of both parameters used to quantify heterogeneity of water flow in soils, we considered different regimes of water flow that could be detected with 10 probes in a given area. First, we assumed that 20, 30, 40, 50, 60, 70, 80, and 90% of water, applied to this area, flowed through the macropores in the neighbourhood of one probe only. As a result, the bypassing ratio BR was 0.2, 0.3, 0.4, 0.5, 0.6, 0.7, 0.8, and 0.9, respectively. Next, we assumed that water flowed preferentially in the neighbourhood of two probes, and 15, 20, 25, 30, 35, 40, and 45% of water, applied to the area, flowed through the macropores in the neighbourhood of each of these two probes. The bypassing ratio BR was thus 0.3, 0.4, 0.5, 0.6, 0.7, 0.8, and 0.9 for this scenario, respectively. Finally, we assumed that water flowed preferentially in the neighbourhood of three probes, and 15, 20, 25, and 30% of water, applied to the area, flowed through the macropores in the neighbourhood of each of these three probes. As a result, the bypassing ratio BR was 0.45, 0.6, 0.75, and 0.9 for the last scenario, respectively. The ECS and DPF parameters were determined for these numerical scenarios.

## RESULTS AND DISCUSSION

### Radioactive tracer experiment

The relative counting rates as a function of depth, measured during the experiment, are presented in Fig. 2. Measurement variability across eight probes is evident in Fig. 2 as each probe detected different transport regime (either in the soil matrix and/or through preferential pathways and other structural soil elements). After irrigation of 200 mm of water, an increase of the counting rates was detected at 80 cm depth (Fig. 2d).

The ECS and DPF parameters at the depth of 30 cm for 4 hours and 10 hours after the tracer application are shown in Fig. 3a and Fig. 3b, respectively. The values of the ECS are similar for these two times; however, the DPF values differ notably. This is caused by different pattern of the FTWC-FCA relationship (as seen in Fig. 3a and 3b) and the fact that the ECS is defined at 90% of FTWC. Conversely, the DPF takes into account the shape of the FTWC-FCA relationship by calculating the shaded area in Fig. 3.

The plot of the DPF against the ECS values is shown in Fig. 4 for four different measurement times (and cumulative water inputs) after the tracer application. This figure is complemented with the DPF-ECS relationship calculated for the scenario assuming preferential flow in the neighbourhood of three probes (cf. Fig. 6c). The trend of both relationships seems similar. The ECS values, calculated for the tracer experiment, range from 0.455 to 0.847  $\text{m}^2 \text{m}^{-2}$  while the values of the DPF are limited in the interval from 0.068 to 0.299 (–). The values of the ECS are spread over the whole range for three measurement times; only the ECS values pertaining to time level  $t = 4$  h lie in a narrow interval (i.e., 0.685–0.847  $\text{m}^2 \text{m}^{-2}$ ). Two outliers can be identified in Fig. 4, at about ECS = 0.8  $\text{m}^2 \text{m}^{-2}$  and DPF = 0.2 (–); these two points are characterized by relatively steep increase of the FTWC-FCA curve.

Furthermore, the values obtained from the radioactive experiment suggest that the ECS decreased and the DPF increased with depth (Fig. 5). This indicates an increase in the heterogeneity of water flow and solute transport with depth. The denser macropore network near the surface (but at the same time relatively homogeneous) resulted in smaller heterogeneity of tracer across the eight probes, while the less dense macropore network resulted in greater heterogeneity of tracer distribution deeper in the soil profile.

### Numerical experiments

The plots of the ECS against BR considering different flow regimes (scenarios with preferential flow in 1, 2, and 3 paths) are shown in Fig. 6a. The relationships between the ECS and BR are non-linear, with a moderate decrease of the ECS in the 0.2 to 0.6 range of BR (this part can be approximated by a line  $y = -0.322x + 0.992$ ,  $R^2 = 0.807$ ) and a steep decrease of the ECS for higher values of BR.

The plots of the DPF against BR considering different flow regimes (scenarios with preferential flow in 1, 2, and 3 paths) are presented in Fig. 6b. The DPF increases linearly with an increase of BR for 1, 2, and 3 preferential paths, respectively. As the slope of these lines (approximately 0.5) is about 1.5-times greater than the slope of the line, which fitted the ECS-BR relationship in the 0.2–0.6 range of the BR, it can be concluded that the DPF is more sensitive to the changes of the BR than the ECS.

The relationship between the DPF and ECS values for three different flow regimes is depicted in Fig. 6c. Similarly to the ECS-BR relationship (Fig. 6a), the DPF-ECS relationship is

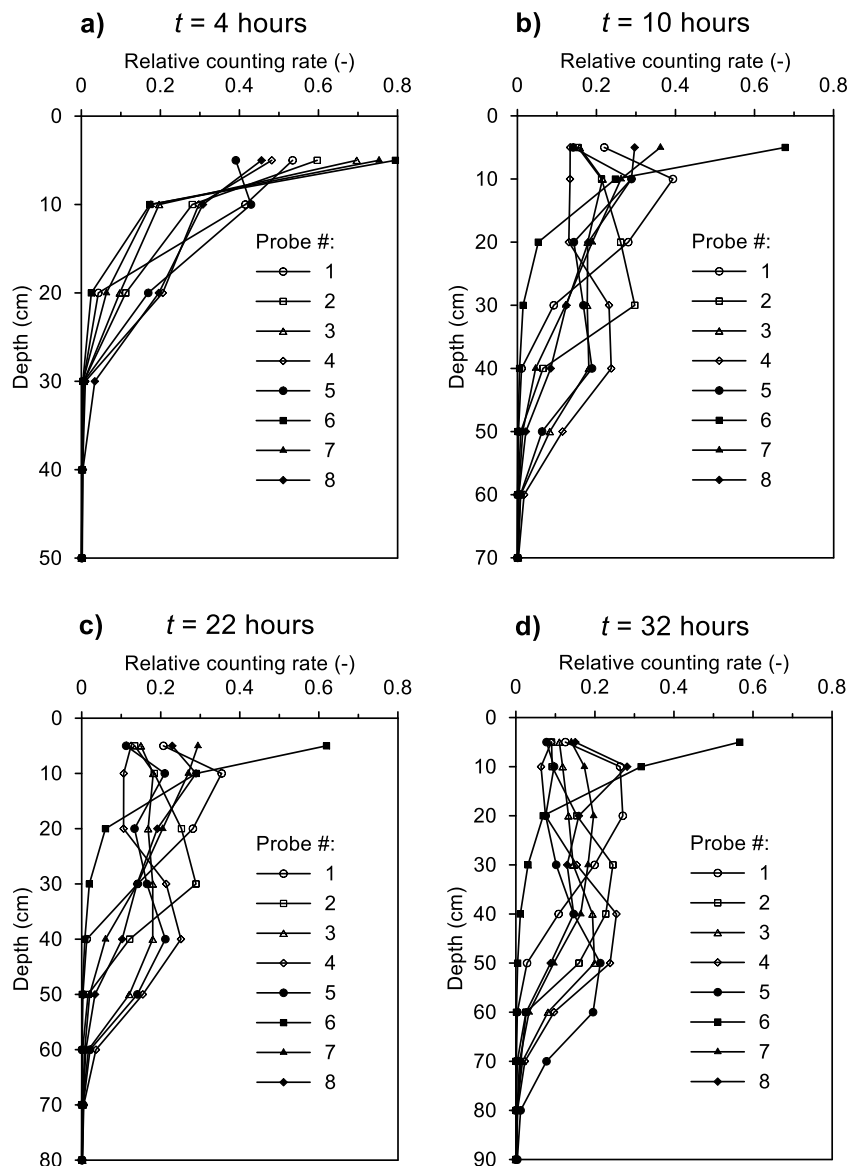


**Fig. 2.** The plots of the relative counting rates against depth for the experiment, measured 4 hours (a), 10 hours (b), 22 hours (c), and 32 hours (d) after the radioactive  $^{131}\text{I}$  tracer application.

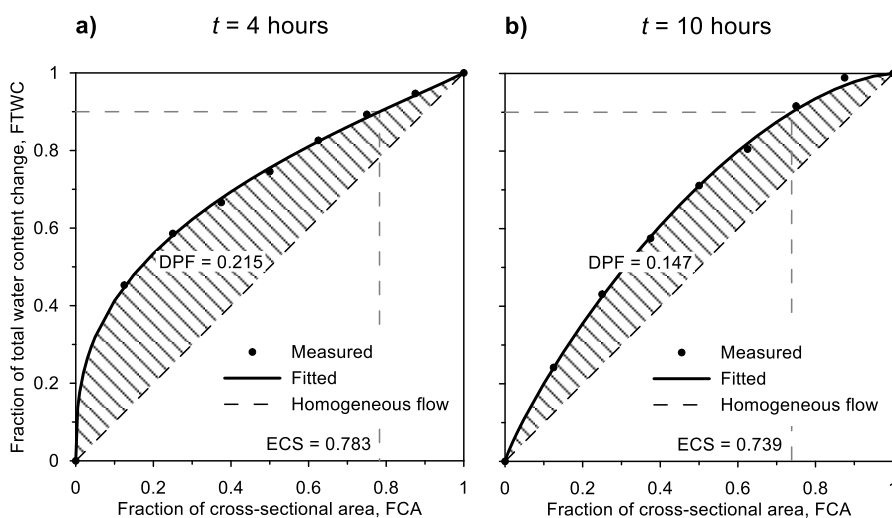


**Fig. 3.** The effective cross section (ECS) and degree of preferential flow (DPF) at the depth of 30 cm for 4 hours (a) and 10 hours (b) after the radioactive  $^{131}\text{I}$  tracer application.

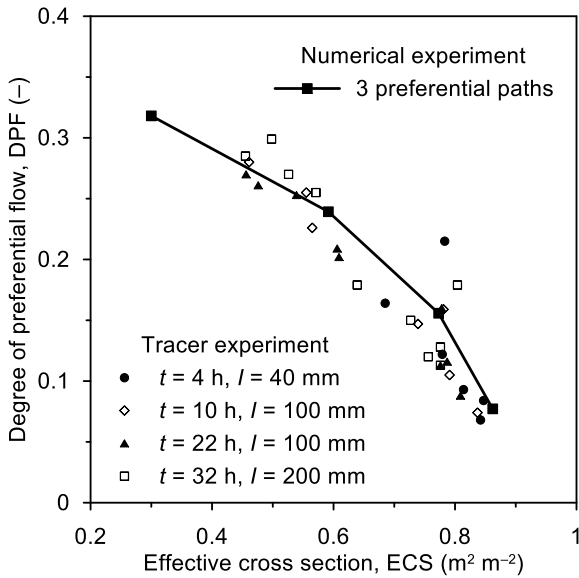


**Fig. 4.** The plots of the degree of preferential flow against the effective cross section for both the radioactive tracer infiltration experiment as a function of water application ( $l$ ) and time from the beginning of tracer application ( $t$ ), and numerical simulation assuming preferential flow in 3 paths (cf. Fig. 6c).

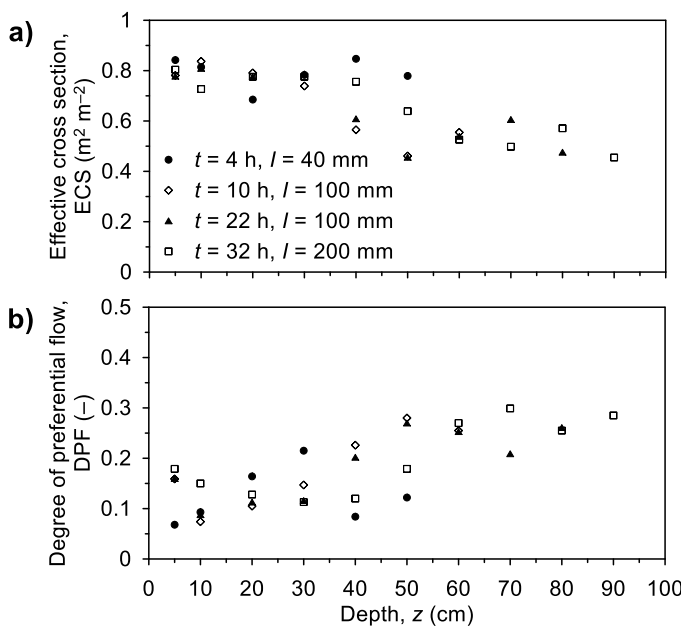


**Fig. 5.** The plot of the effective cross section (a) and the degree of preferential flow (b) as a function of depth  $z$  calculated for the radioactive tracer infiltration experiment.

non-linear, with a moderate decrease of the DPF in the 0.2 to 0.6 range of ECS followed with a steep decrease of the DPF for higher values of ECS. The results of the numerical experiments shown in Fig. 6c can be compared with the DPF-ECS relationship obtained for the radioactive tracer experiment (Fig. 4). The steep decrease of the DPF for higher values of ECS is, however, not seen for the tracer experiment. This suggests that the flow regime during the tracer experiment was less homogeneous than the regime assumed in the numerical experiments.

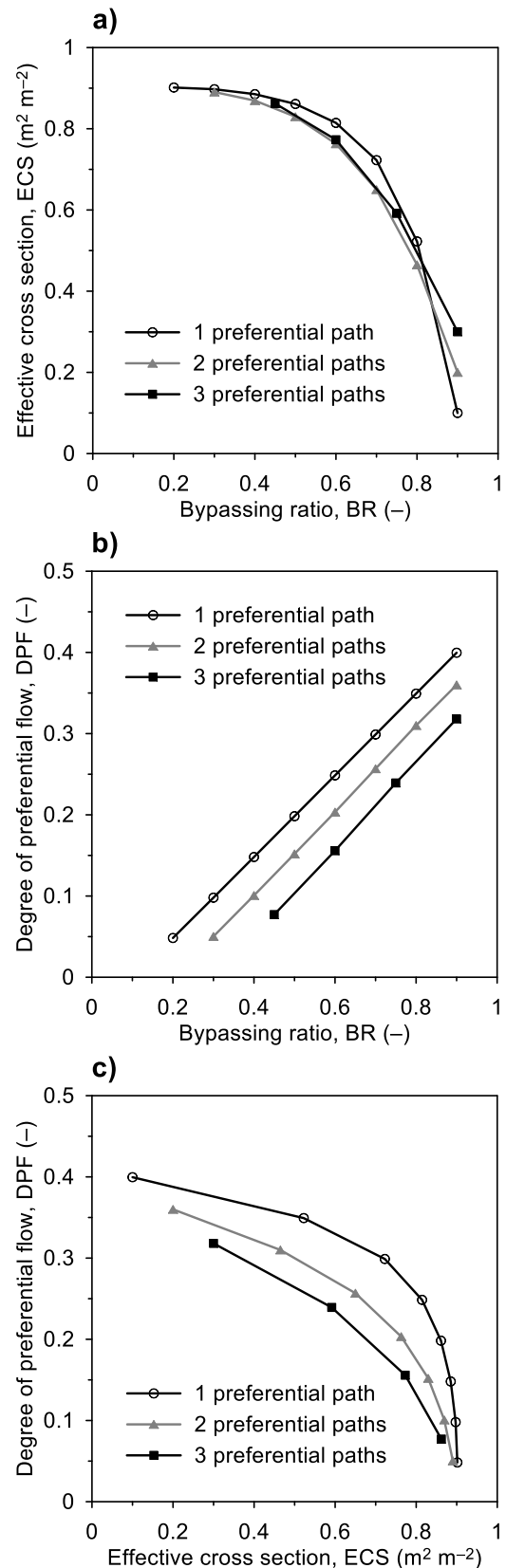


**Fig. 6.** The results of numerical simulation assuming different flow regimes (degree of water flow heterogeneity in the soil as a result of preferential flow in 1, 2, and 3 paths): (a) The plots of the effective cross section against bypassing ratio. (b) The plots of the degree of preferential flow against bypassing ratio. (c) The plots of the degree of preferential flow against the effective cross section.

## CONCLUSIONS

Both the effective cross section (ECS) and the degree of preferential flow (DPF) were found useful to assess the heterogeneity of water flow in the studied soil. For the data from a field tracer experiment, the ECS decreased and the DPF increased with depth, which suggests an increase in the degree of heterogeneity of water flow with depth. Numerical experiments suggest that the ECS decreases non-linearly and the DPF increases linearly with an increase in the bypassing ratio. The DPF was found to be more sensitive to different flow and transport regimes than the ECS. The plot of the DPF against ECS values calculated from the field tracer experiment was consistent with the relationship obtained by the numerical simulation assuming preferential flow in the neighbourhood of three probes. The use of the ECS and DPF parameters to evaluate field experiments with different flow regimes (ranging from homogeneous to highly heterogeneous) is recommended.

*Acknowledgement.* This work was supported by the Scientific Grant Agency VEGA Project No. 2/0073/11. Additional support was provided by the Ministry of Education of the Czech Republic (MSM 6840770002). This publication is the result of the project implementation ITMS 26240120004 Centre of excellence for integrated flood protection of land supported by the Research & Development Operational Programme funded by the ERDF.

## REFERENCES

- Alaoui, A.M., Germann, P., Lichner, L., Novák, V., 1997. Preferential transport of water and <sup>131</sup>Iodide in a clay loam assessed with TDR-technique and boundary layer flow theory. *Hydrol. Earth Syst. Sci.*, 1, 813–822.
- Behrens, H., 1982. New insights into the chemical behaviour of radioiodine in aquatic environments. In: Proc. Int. Conf. Environmental migration of long-lived radionuclides. IAEA, Vienna 1982, pp. 27–40. (IAEA-SM-257/36)
- Bouma, J., Dekker, L.W., Wösten, J.H.M., 1978. A case study on infiltration into dry clay soil. II. Physical measurements. *Geoderma*, 20, 41–51.
- Dohnal, M., Dušek, J., Vogel, T., Císlarová, M., Lichner, L., Štekauerová, V., 2009. Ponded infiltration into soil with biopores – field experiment and modeling. *Biologia*, 64, 580–584.
- Edwards, W.M., Shipitalo, M.J., Owens, L.B., Dick, W.A., 1993. Factors affecting preferential flow of water and atrazine through earthworm burrows under continuous no-till corn. *J. Environ. Qual.*, 22, 453–457.
- Faško, P., Lapin, M., Pecho, J., 2008. 20-year extraordinary climatic period in Slovakia. *Meteorolog. Cas.*, 11, 99–105.
- Flury, M., Flühler, H., Jury, W.A., Leuenberger, J., 1994. Susceptibility of soils to preferential flow of water: A field study. *Water Resour. Res.*, 30, 1945–1954.
- Hardy, J.T., 2003. *Climate Change. Causes, Effects, and Solutions.* Wiley, Chichester, 247 pp.
- Homolák, M., Capuliak, J., Pichler, V., Lichner, L., 2009. Estimating hydraulic conductivity of a sandy soil under different plant covers using minidisk infiltrometer and a dye tracer experiment. *Biologia*, 64, 600–604.
- Kneale, W.R., White, R.E., 1984. The movement of water through cores of a dry (cracked) clay-loam grassland topsoil. *J. Hydrol.*, 67, 361–365.
- Lichner, L., 1990. A method for measurement of water infiltration rate into unsaturated soil. Czechoslovak Patent No. 263025. Federal Bureau for Inventions, Prague. (In Czech.)
- Lichner, L., 1992. Laboratory and field measurements of solute transport in soils by means of nuclear tracer technique. *Vodohosp. Čas.*, 40, 548–561.
- Lichner, L., 1995. A nuclear tracer technique for investigation of solute transport in the unsaturated zone of soil. In: Leibundgut, Ch. (ed.): Proc. Int. Symp. Tracer technologies for hydrological systems, Boulder 1995. IAHS Publication No. 229, Wallingford, pp. 109–116.
- Lichner, L., 1997. In-situ measurement of bypassing ratio in macroporous soil. *J. Hydrol. Hydromech.*, 45, 365–376.
- Lichner, L., Capuliak, J., Zhukova, N., Holko, L., Czachor, H., Kollár, J., 2013. Pines influence hydrophysical parameters and water flow in a sandy soil. *Biologia*, 68, 1104–1108.
- Lichner, L., Eldridge, D.J., Schacht, K., Zhukova, N., Holko, L., Šír, M., Pecho, J., 2011. Grass cover influences infiltration into a sandy soil. *Pedosphere*, 21, 719–729.
- Lichner, L., Mészáros, I., Germann, P., Alaoui, A.M., Šír, M., Faško, P., 1999. Impact of land-use change on nutrient fluxes in structured soils. In: Heathwaite, L. (ed.): Proc. Int. Symp. Impact of land-use change on nutrient loads from diffuse sources, Birmingham 1999. IAHS Publication No. 257, Wallingford, pp. 171–177.
- Pekárová, P., Svoboda, A., Miklánek, P., Škoda, P., Halmová, D., Pekár, J., 2012. Estimating flash flood peak discharge in Gidra and Parná basin: case study for the 7–8 June 2011 flood. *J. Hydrol. Hydromech.*, 60, 206–216.
- Seki, M., Oikawa, J., Taguchi, T., Ohnuki, T., Muramatsu, Y., Sakamoto, K., Amachi, S., 2013. Laccase-catalyzed oxidation of iodide and formation of organically bound iodine in soils. *Environ. Sci. Technol.*, 47, 390–397.
- Shetaya, W.H.A.H., 2011. Iodine dynamics in soil. Ph.D. Thesis. University of Nottingham, Nottingham, 171 pp.
- Shipitalo, M.J., Dick, W.A., Edwards, W.M., 2000. Conservation tillage and macropore factors that affect water movement and the fate of chemicals. *Soil Till. Res.*, 53, 167–183.
- Smettem, K.R.J., 2009. The relation between runoff generation and temporal stability of soil macropores in a fine sandy loam. *Biologia*, 64, 470–473.
- Soil Survey Division Staff, 1993. *Soil survey manual.* Soil Conservation Service. U.S. Department of Agriculture Handbook 18, 437 pp.
- Täumer, K., Stoffregen, H., Wessolek, G., 2006. Seasonal dynamics of preferential flow in a water repellent soil. *Vadose Zone J.*, 5, 405–411.
- Vogel, T., Lichner, L., Dusek, J., Cipakova, A., 2007. Dual-continuum analysis of cadmium tracer field experiment. *J. Contam. Hydrol.*, 92, 50–65.
- WRB, 2006. *World reference base for soil resources 2006.* 2nd edition. World Soil Resources Reports No. 103. FAO, Rome, 128 pp.

Received 24 April 2013  
Accepted 13 August 2013